Published in final edited form as:

Free Radic Biol Med. 2014 April ; 69: 265–277. doi:10.1016/j.freeradbiomed.2014.01.030.

Redox Properties of Human Hemoglobin in Complex with Fractionated Dimeric and Polymeric Human Haptoglobin

Todd L. Mollan[a], **Yiping Jia**[a], **Sambuddha Banerjee**[b], **Gang Wu**[c], **R. Timothy Kreulen**[b], **Ah-Lim Tsai**[c], **John S. Olson**[d], **Alvin L. Crumbliss**[b], and **Abdu I. Alayash**[a,*]

[a]Laboratory of Biochemistry and Vascular Biology, Division of Hematology, Center for Biologics Evaluation and Research, Food and Drug Administration, Bethesda, Maryland 20852, United States

[b]Department of Chemistry, Duke University, Durham, North Carolina 27708, United States

[c]Hematology Division, Department of Internal Medicine, University of Texas-Houston Medical School, Houston, Texas 77030, United States

[d]Biochemistry and Cell Biology Department, Rice University, Houston, Texas 77251, United States

Abstract

Haptoglobin (Hp) is an abundant and conserved plasma glycoprotein, which binds acellular adult hemoglobin (Hb) dimers with high affinity and facilitates their rapid clearance from circulation following hemolysis. Humans possess three main phenotypes of Hp, designated Hp 1-1, Hp 2-1, and Hp 2-2. These variants exhibit diverse structural configurations and have been reported to be functionally non-equivalent. We have investigated the functional and redox properties of Hb-Hp complexes prepared using commercially fractionated Hp and found that all forms exhibit similar behavior. The rate of Hb dimer binding to Hp occurs with bimolecular rate constants of ~0.9 $\mu M^{-1}s^{-1}$, irrespective of the type of Hp assayed. Although Hp binding does accelerate the observed rate of HbO_2 autooxidation by dissociating Hb tetramers into dimers, the rate observed for these bound dimers is 3- to 4-fold slower than that of Hb dimers free in solution. Co-incubation of ferric Hb with any form of Hp inhibits heme loss to below detectable levels. Intrinsic redox potentials ($E_{1/2}$) of the ferric/ferrous pair of each Hb-Hp complex are similar, varying from +54 to +59 mV (vs NHE), and are essentially the same as reported by us previously for Hb-Hp complexes prepared from unfractionated Hp. All Hb-Hp complexes generate similar high amounts of ferryl Hb following exposure to hydrogen peroxide. EPR data indicate that the yields of protein-based radicals during this process are approximately 4% to 5%, and are unaffected by the variant of Hp assayed. These data indicate that the Hp fractions examined are equivalent to each

*Correspondence to: Abdu I. Alayash, Ph.D., D.Sc., Laboratory of Biochemistry and Vascular Biology, Center for Biologics Evaluation and Research, Food and Drug Administration, NIH Bldg. 29, Rm. 112, 8800 Rockville Pike, Bethesda, Maryland 20892, Phone: 301/827-3813, Fax: 301/435-4034, abdu.alayash@fda.hhs.gov.

The authors declare no competing financial interest.

other with respect to Hb binding and associated stability and redox properties, and that this result should be taken into account in the design of phenotype-specific Hp therapeutics aimed at countering Hb-mediated vascular disease.

Keywords

EPR; ferryl; haptoglobin; heme loss; Hemoglobin A (HbA); iron(IV) oxo; protein-based radical; redox potential; spectroelectrochemistry; sulfhemoglobin

INTRODUCTION

Hemoglobin (Hb) is an abundant and conserved metalloprotein which is the primary dioxygen (O_2) transporter in many organisms [1]. Adult human Hb consists of two alpha (α) subunits and two beta (β) subunits, each of which are held together non-covalently and contain a single, iron(Fe)-containing protoporphyrin IX prosthetic group [1]. Hb is redox active, especially when released from the reducing environment of erythrocytes during normal and aberrant hemolysis [2]. For example, autooxidation of oxyhemoglobin (HbO_2) or oxymyoglobin (MbO_2) produces met-Hb or met-Mb, respectively, and superoxide radicals ($O_2^{\bullet -}$, $HO_2^{\bullet}$) via electron transfer [3,4]. Superoxide spontaneously dismutates into O_2 and hydrogen peroxide (H_2O_2), which can then react with Fe(II) or Fe(III) within Hb to produce ferryl Hb (Fe(IV)oxo species; e.g., $Fe^{4+}{=}O^{2-}$) [5]. In the case of reaction with Fe(III), a protein-based radical is additionally formed (i.e., $Y^{\bullet}$-$Fe^{4+}{=}O^{2-}$) [5]. Ferryl Hb, protein-based radicals, and H_2O_2 can all oxidize biological substrates in vivo, including Hb itself, and these reactions have been implicated in diverse pathophysiologies [2].

Haptoglobin (Hp) is a Hb-scavenging plasma glycoprotein which binds non-covalently to hemoglobin dimers that are generated by dissociation of acellular Hb tetramers after hemolysis [6]. Hp has been shown to reduce the oxidative toxicity of acellular Hb in part by facilitating its rapid removal from circulation through CD163-receptor-mediated endocytosis [7,8]. Additionally, Hp binding impedes the renal clearance of Hb [9], dramatically diminishes the rate of heme dissociation from ferric Hb dimers [10–12], and reduces Hb-mediated bacterial pathogenesis in vivo, likely through impaired bacterial iron acquisition from free heme [13]. In addition, we have shown that Hp binding considerably alters the intrinsic redox properties of bound Hb dimers [14,15]. These findings suggest roles for Hp in iron and Hb homeostasis, anti-oxidant behavior, immune function, and possibly other processes [6,9,16].

The gene which codes for Hp in humans exists in three main isoforms: Hp^{1F}, Hp^{1S}, and Hp^{2} [17]. Each isoform generates a single polypeptide which is cleaved into one Hp alpha (α) subunit (9–17 kDa) and one glycosylated Hp beta (β) subunit (34–39 kDa) [6,17]. The α subunits derived from Hp^{1F} and Hp^{1S} (α^1 subunits) possess slightly different amino acid compositions that result in either fast(α^{1F})- or slow(α^{1S})-migrating electrophoretic species [17]. Those derived from Hp^{2} (α^2 subunits) are believed to migrate uniformly [17]. Hp β subunits are the site of non-covalent binding of Hb dimers [6,7]. In mature human Hp, these α and β subunits are thought to be assembled through disulfide linkages into the following configurations: (a) Hp 1-1, which has the formula $(\alpha^1\beta)_2$; (b) Hp 2-1, which has the formula

$(\alpha^1\beta)_2(\alpha^2\beta)_n$ and possibly others; and (c) Hp 2-2, which has the formula $(\alpha^2\beta)_n$, where n indicates a variable number of repeats of the Hp αβ protomer [6]. Individuals with wild-type *Hp* genetic loci bear only one of these three Hp variants, although different configurations of Hp α^{1F} and α^{1S} subunits occur within each protein [6]. Other variants have also been identified in some populations [6].

Hp 1-1, Hp 2-1, and Hp 2-2 have been associated with widely differing biological activities in vivo [16]. For example, Hp 2-2 has been associated with an increased susceptibility to diabetic cardiovascular disease; uptake of Hb-Hp(1-1) complexes by CD163 receptors is reportedly faster and its binding results in increased concentrations of anti-inflammatory mediators than Hb-Hp(2-2) complexes; and the angiogenic potency of Hp 2-2 is reportedly greater than that of Hp 1-1 [18]. Many other differences between the in vivo behavior of Hp 1-1 and Hp 2-2 have also been suggested [16,18]. However, there is a dearth of mechanistic studies that have attempted to address the biochemical basis of these differences. To investigate and better understand the effects exerted by human Hp on Hb following binding, we studied Hb dimers in complex with: (a) unfractionated Hp, which consists of a mixture of Hp 1-1, Hp 2-1, and Hp 2-2; (b) fractionated, dimeric Hp (i.e., Hp 1-1); and (c) fractionated, polymeric Hp (i.e., predominantly Hp 2-2, with minor amounts of Hp 2-1). We previously reported that unfractionated Hp binding alters the oxygenation and oxidation states of the Hb iron [15,19]. To examine the effects of Hp heterogeneity, we complexed both ferrous and ferric Hbs with unfractionated Hp and its fractionated forms in an experiment-specific fashion to approximate the experimental conditions reported earlier for studies using unfractionated Hp [15]. We report that Hb-Hp binding kinetics, hydrogen-peroxide-driven oxidative transitions of the heme iron, radical formation, heme loss rates, and intrinsic redox potentials are all similar among the different forms of Hp-Hb complexes examined.

MATERIALS AND METHODS

Protein purification, handling, sample preparation

Fractionated dimeric and polymeric Hp were provided by Bio Products Laboratory, Ltd. (BPL; Hertfordshire, UK) [20]. These samples were obtained by purifying human Hp from pooled donated plasma and then separating the Hp variants by size exclusion chromatography. Although much of the Hp 2-1 was removed from the polymeric Hp fraction, small amounts of Hp 2-1 trimers, which are similar in size to Hp 2-2 polymers, co-purified in the polymer fraction. Purity was verified by native polyacrylamide gel electrophoresis using a NativePAGE Novex 4–16% Bis-Tris gels in an Invitrogen electrophoresis apparatus (Carlsbad, California, US). Human Hb was derived from whole blood, which was collected with informed consent in accordance with an IRB-approved protocol at the National Institutes of Health (Bethesda, Maryland, US). Recombinant mutant H64Y/V68F sperm whale apo Mb was produced and purified as previously reported [21].

Hb was purified from whole blood using established methods [22]. Following the completion of these steps, erythrocyte catalase was removed using an ÄKTA FPLC system and an XK 16/70 column containing Superdex 200 media or an XK 50/100 column containing Sephacryl 200 media (GE Healthcare Bio-Sciences Corporation, Piscataway,

New Jersey, US). The volume of the samples loaded onto these columns was <1% of the column bed volume, sample concentrations for each injection were <60 mg/mL, and flow rates were set to 1.0 mL/minute. Samples were pre-filtered through syringe filters with a 0.45 μm pore size and 25 mm diameter prior to application to the columns (EMD Millipore, Billerica, Massachusetts, US). All Hb purification steps were performed at 4°C using 20 mM or 50 mM potassium phosphate buffer, pH 7.0 at 22°C. Elution of protein was monitored by optical absorbance at 280 nm. Because human Hb and catalase have relative molecular masses of approximately 64.5 kDa and 220 kDa, respectively [23,24], catalase elutes before Hb. Catalase activity assays [25] performed on Hb samples before and after this gel filtration step indicated that the enzyme was removed to levels that were below the detection limit of this assay. Following catalase removal, samples were re-concentrated at 4°C to approximately 1.5 mM in heme equivalents using Centricon Centrifugal Filter Devices (EMD Millipore, Billerica, Massachusetts, US). Hb samples were stored at −80°C when not in use. Hp was stored at 4°C when not in use.

The molar extinction coefficients used to calculate Hb concentrations in heme equivalents were: 15.2 $mM^{-1}cm^{-1}$ at 576 nm for $Hb(O_2)$ and 4.4 $mM^{-1}cm^{-1}$ at 631 nm for ferric Hb using 50 mM potassium phosphate buffer, pH 7.0 at 22°C, in both cases [26,27]. The concentrations of all Hb-containing solutions are given in heme equivalents. Mass concentrations in milligrams of Hp per milliliter of buffer solution were provided by BPL. In fluorescence emission stopped-flow measurements of Hb-Hp binding, as well as in the ferryl species quantification assays using disodium sulfide (Na_2S), relative molecular masses of 43 kDa and 49.8 kDa for Hp 1-1 and Hp 2-2, respectively, were used in conjunction with BPL-provided mass concentrations (bicinchoninic acid assay) to estimate the molarity of Hb dimer binding sites in a given Hp stock solution (i.e., the molarity of Hp αβ dimers). These values are based on the work of Kurosky et al. [28], although there are conflicting values elsewhere in the literature [6]. In the spectroelectrochemical, H_2O_2-induced radical formation, and heme loss studies, HbO_2-Hp complexes were prepared by adding significant molar excesses of HbO_2 to solutions of Hp using concentrations that were estimated using the above methods. The resulting samples were incubated on ice for ~10 minutes and then fractionated by size exclusion chromatography using either a 10/300 GL column containing Superose 12 for volumes of less than 100 μL or an XK 16/70 column containing Superdex 200 media for larger volumes (GE Healthcare Bio-Sciences Corporation, Piscataway, New Jersey, US). Sample volumes, concentrations, flow rates, and buffers were the same as described above for catalase removal. The peaks that elute first correspond to HbO_2-Hp complexes (≥ 150 kDa), and are followed by unbound tetrameric HbO_2 (~64.5 kDa). This method results in a population of Hp that has all of its Hb αβ dimer binding sites occupied, with no excess HbO_2 present in solution. Individual samples were re-concentrated as necessary at 4°C using Centricon Centrifugal Filter Devices (EMD Millipore, Billerica, Massachusetts, US).

Where indicated, Hb and Hb-Hp complexes (met-Hb and met-Hb-Hp, respectively) were generated by adding 10-fold or greater molar excesses of potassium ferricyanide from a 20 mM stock solution to each sample and incubating them on ice for approximately five minutes before applying the samples to an XK 16/20 column containing approximately 30 mL of Sephadex G-25 media or a gravity-fed disposable PD-10 desalting column with a ~10

mL bed volume (GE Healthcare Bio-Sciences Corporation, Piscataway, New Jersey, US). Conversion from the Fe(II) to the Fe(III) state could be followed visually by observing the samples' color change from red to brown. The stock solution of potassium ferricyanide was prepared and the concentration estimated by dry weight. Sample loading volumes for this step were less than 2 mL, concentrations in heme equivalents were less than 1.5 mM, and the buffer used was 50 mM potassium phosphate buffer, pH 7.0 at 22°C unless otherwise indicated.

Heme-free H64Y/V68F Mb (apoMb) was prepared using the butanone method of Ascoli et al. [29] An extinction coefficient of 15.2 $mM^{-1}cm^{-1}$ at 280 nm was used to determine the molar concentration of apoMb [21].

Rapid Mixing Experiments

Fluorescence emission stopped-flow experiments were conducted using an Applied Photophysics SX-17 microvolume stopped-flow spectrophotometer equipped with a refrigerated water circulator bath for temperature control (Leatherhead, Surry, UK). The instrument was configured as follows: Excitation path length, 10 mm; entrance and exit slit widths, 0.5 mm (i.e., 2.3 nm spectral bandwidth); excitation wavelength, 285 nm; cutoff filter, 360 nm; and shot volume, 100 μL. The volume of the cell was 20 μL and the photomultiplier unit was positioned at a 90° angle from the incident light. The fluorescence cell dimensions were 10 × 2 × 1 mm. The refrigerated water circulator bath was set to 22 °C for all experiments and at least three time courses were accumulated and averaged for each data set.

Autooxidation and Heme Loss

Autooxidation experiments were carried out by incubating HbO_2 in 50 mM KP_i at pH 7.4, 37 °C, and then recording visible spectra (350 nm to 700 nm) every 5 minutes for 16 hours. Experiments were performed at five different total HbO_2 concentrations, ranging from 2.5 to 100 μM in heme equivalents, in the absence or presence of 1 αβ equivalent of Hp1-1 per Hb dimer. Then time courses at a fixed wavelength were fitted to either single or two-exponent expressions with an offset using Equation 1.

$$y=y_\infty+y_1\exp(-k_1t)+y_2\exp(-k_2t) \quad \text{Eq. 1}$$

where y is the observed absorbance reading as a function of time, y_∞ is the absorbance value at infinite time, y_1 and y_2 are the absorbance changes associated with the fast and slow phases, and k_1 and k_2 are the fast and slow first-order observed rate constants. When fitting to a single-exponent, y_2 was set equal to zero and not allowed to vary. In some cases the final absorbance value after complete autooxidation, $y_{\infty,}$ was difficult to determine independently when the reaction was very slow, particularly for high concentrations of free HbO_2. However, the value of y_∞ for free HbO_2 tetramers could be obtained from the fitted values for the Hp(dimer)-HbO_2 experiment at exactly the same protein concentration because, in this case, the rate was 3- to 4-fold greater and the endpoint was well defined.

Heme loss rates from met-Hb alone and in complex with Hp were measured using the method of Hargrove et al. [21]. In these experiments, spectra between 400 nm and 700 nm were recorded every minute for 4 hours at 37 °C using 200 mM potassium phosphate buffer, 600 mM sucrose, prepared at pH 7.0 at 22 °C. Concentrations of Hb and Hb-Hp complexes in heme equivalents were 2.5 μM, and the concentration of H64Y/V68F apoMb was 20 μM. Total reaction volumes of 1.0 mL were prepared by placing 800 μL of the buffer into each cuvette for thermal equilibration at 37 °C prior to the start of data collection. This 800 μL volume contained met-Hb or met-Hb-Hp complex at a concentration such that dilution to 1.0 mL would give a final concentration of 2.5 μM in heme equivalents. Following thermal equilibration, 200 μL of a pre-prepared stock solution of H64Y/V68F apoMb was quickly added to each of the cuvettes to give a final concentration of 20 μM following dilution to 1.0 mL. Data collection was then started.

Spectroelectrochemistry

The intrinsic redox potentials of fractionated Hp samples complexed with human Hb were recorded under anaerobic conditions in 200 mM potassium phosphate buffer, pH 7.2 at 22°C, using $[Ru(NH_3)_6]Cl_3$ as mediator in a three electrode set up (platinum mesh working electrode, platinum wire auxiliary electrode, and Ag/AgCl reference electrode) [30–32]. Before starting the potential sweep the protein sample was degassed and purged with argon, and throughout the experiments, the protein solution was maintained under positive argon pressure to avoid oxygenation. The final concentration of the protein in solution was 0.08 mM in heme equivalents and that of the mediator was 0.8 mM. All potentials reported are relative to the normal hydrogen electrode (NHE). UV-Vis absorbance spectra were recorded with a Cary Bio 100 spectrophotometer and the potential scans were performed using an EG & G Princeton Applied Research Model 863 potentiostat. Prior to voltage scanning the protein solution was subjected to a high positive potential to convert all the deoxygenated bound Hb dimers into met-Hb as indicated by a steady Soret band at 405 nm. Once this steady band at 405 nm was obtained, implying the conversion of all the Hb to the Fe(III) state, the potential of the platinum working electrode was made progressively negative producing more and more Fe(II)Hb absorbing at 430 nm. The protein solution was allowed to equilibrate at each applied potential (E_{app}) for ~15 minutes to reach a steady state absorbance. The potential sweep in the negative direction was continued until the absorbance at 430 nm reached a maximum as a function of the potential scan indicating conversion of all Hb to the Fe(II) state. At the end of each experiment, the direction of the potential scan was reversed from negative to positive to establish the reversibility of the process.

The differences in absorbance for the Soret bands (405 nm for Fe(III)-heme and 430 nm for Fe(II)-heme) at each applied potential are related to the relative concentrations of each species through Beer's law [30–32]. Once the respective concentrations were determined, log[Ox]/[Red] was plotted as a function of the applied potential (after conversion to NHE scale) according to the Nernst equation:

$$E_{applied} = E_{\frac{1}{2}} + \frac{RT}{nF} \log\left(\frac{[Hb_{ox}{:}Hp]}{[Hb_{red}{:}Hp]}\right) \quad \text{Eq. 2}$$

where $E_{applied}$ is the applied potential at each data point, $E_{½}$ is the redox potential when [Hb_{red}:Hp] = [Hb_{ox}:Hp], R is the universal gas constant, T is the absolute temperature, n is the number of electrons transferred in an ideal Nernstian system, F is the Faraday constant, and $[Hb_{red}:Hp]$ and $[Hb_{ox}:Hp]$ are the concentrations of the Fe(II)- and Fe(III)-bearing Hb-Hp complexes, respectively. Horse heart Mb was used as a standard for calibration purposes (Sigma-Alrich, Saint Louis, Missouri, US).

Ferryl Hb species stability within the complex

H_2O_2-induced ferryl Hb species were detected using a Cary 100 visible light optical absorbance spectrophotometer (Agilent Technologies, Santa Clara, California, US) and the following previously-described method [33]. A stock solution of met-Hb was prepared and its concentration calculated using appropriate molar extinction coefficients. Then the following four samples were prepared in 20 mM potassium phosphate buffer, pH 7.4 at 22°C, pre-chilled to 4°C: (a) 10 μM metHb and 20 μM H_2O_2 in a volume of 9 mL of buffer; (b) 10 μM met-Hb premixed with 20 μM unfractionated Hp and then reacted with 20 μM H_2O_2 in a volume of 9 mL of buffer; (c) 10 μM met-Hb premixed with 20 μM Hp(dimer) and then reacted with 20 μM H_2O_2 in a volume of 9 mL of buffer; and (d) 10 μM met-Hb premixed with 20 μM Hp(polymer) and then reacted with 20 μM H_2O_2 in a volume of 9 mL of buffer. Hp concentrations were calculated based on mass concentrations of Hp stock solutions and the molecular masses of each form of Hp (see above). The concentration of unfractionated Hp was calculated using supplied mass concentrations and an approximate molecular mass of 46.4 kDa. A 16.6 mM stock solution of H_2O_2 was used for the H_2O_2 additions, and this stock solution was prepared using unbuffered H_2O and an extinction coefficient at 240 nm of 43.6 $M^{-1}cm^{-1}$ for H_2O_2 [34]. Sample preparation was done as quickly as possible, with H_2O_2 being added to the complexes immediately before mixing by inversion and starting a timer. At time points of 2 minutes, 45 minutes, and 90 minutes post-H_2O_2-addition, 1 mL samples were withdrawn in triplicate from each of the four sample tubes and were transferred to smaller tubes containing catalase to give a final concentration of 200 units of activity per mL in each 1 mL sample (Sigma-Aldrich, Saint Louis, Missouri, US). Samples were incubated on ice for 30 seconds to allow the catalase to degrade any remaining H_2O_2. Then, 20 μM disodium sulfide (Na_2S) was added to each tube and mixed by inversion. Visible light optical absorbance spectra were recorded for each sample between 500 nm and 700 nm. A stock solution of 2 mM Na_2S in H_2O was prepared for this purpose by dry weight using a molar mass of 78.0 g/mol for Na_2S. Spectra for each sample were plotted following the completion of the experiment and sulfhemoglobin (sulf-Hb) concentrations were calculated using an extinction coefficient of 24.0 $mM^{-1}cm^{-1}$ at 617 nm [33].

Electron Paramagnetic Resonance

H_2O_2-induced radical formation was investigated using a previously reported method [35]. Briefly, the HbO_2 and HbO_2-Hp samples were oxidized to met-Hb and met-Hb-Hp complexes using excess potassium ferricyanide as described above. For measurements made in the liquid He temperature range, sample concentrations were measured spectrophotometrically following oxidation to the ferric state, and were determined to be: (1) Hb = 1,200 μM; (2) Hb-Hp(unfrac) = 600 μM; (3) Hb-Hp(dimer) = 189 μM; and (4) Hb-

Hp(poly) = 380 μM. For the measurements made in the liquid nitrogen temperature range, all samples were diluted to 390 μM, except for the Hb-Hp(polymer) sample which was used at a concentration of 290 μM due to sample limitation. In the experiments conducted using liquid nitrogen, HbO_2 was oxidized to the ferric state prior to Hb-Hp complex preparation, whereas in the liquid helium experiments the complexes were oxidized after complex formation. Ferric samples were treated on ice with either 1-, 1.5-, or 5-fold molar excesses of H_2O_2 for the indicated times before quickly freezing them in a dry-ice-ethanol bath prior to recording spectra. EPR spectra were recorded using a Bruker EMX spectrometer equipped with a liquid helium continuous flow cryostat connected with a GFS600 transfer line and an ITC503 temperature controller (Oxford Instruments, Abingdon, Oxon, UK). The experimental parameters are provided in the figure legend accompanying each data set.

Reagents

Reagents were purchased from Sigma-Aldrich (Saint Louis, Missouri, US) or Fisher Scientific (Pittsburgh, Pennsylvania, US). Bovine liver catalase was purchased from Sigma-Aldrich (C100-50MG), and its functional activity was verified using established methods prior to its use [25].

Fitting

Where indicated, data were fit using Excel Solver (Microsoft Corp., Redmond, Washington, US) and a nonlinear regression method described elsewhere [36].

RESULTS

Hp purity and verification of fractions

The purity of Hp fractions obtained from BPL was investigated using blue native polyacrylamide gel electrophoresis. Figure 1 depicts a representative gel containing samples of unfractionated Hp, dimeric Hp and polymeric Hp in lanes 2, 3, and 4, respectively. Although the relative migration patterns of these samples agree with previous reports [16], the estimated molecular masses of each Hp variant are shifted to higher values, possibly due to the effects of Hp glycosylation of the Hp β subunits. These data indicate that the Hp fractionation results in efficient separation of the different forms of Hp.

Hb-Hp association rates

Hp binds HbO_2 with a stoichiometry of one HbO_2 dimer to one Hp αβ dimer [16]. The stoichiometry of this interaction is believed to be equivalent for the different forms of Hp [6], and the binding affinity has been examined previously by analytical ultracentrifugation [37], electrophoresis [37,38], calorimetry [39], and fluorescence quenching [37,40] methods. These studies suggest that the equilibrium dissociation constant (K_D) is immeasurably low [37,39] and $\leq 10^{-15}$ M [40]. The rate constant for the association of Hp with HbO_2 dimers was first examined by Nagel and Gibson [41,42], and subsequently Alfson et al. [43] and Cohen-Dix et al. [44]. These investigators used rapid mixing fluorescence emission spectrophotometry to monitor complex formation. They reported that, upon excitation with light of a wavelength of ~285 nm, Hp exhibits intrinsic fluorescence with an emission maximum at a wavelength of ~350 nm [41]. This fluorescence emission maximum is

quenched upon interaction with all forms of Hb, and this fluorescence decrease is a direct measure of Hb-Hp complex formation [41–43]. We applied this method to probe for differences between the rates of Hb-Hp complex formation using unfractionated Hp, dimeric Hp, and polymeric Hp.

As shown in Figure 2A, rapid mixing of 80 μM HbO_2 in heme equivalents with 0.1 mg/mL unfractionated Hp, dimeric Hp, or polymeric Hp (pre-mixing concentrations) in air-equilibrated buffer results in the quenching of Hp intrinsic fluorescence on time scales of several seconds. In this experiment, we report Hp mass concentrations instead of molarities because conflicting reports exist as to the molecular masses of the different forms of Hp [6]. However, approximations of the dimeric and polymeric Hp molarities in Hp αβ protomer equivalents can be calculated assuming molecular masses of 43 kDa and 49.8 kDa for these species, respectively [28]. Using these values, the molarities of dimeric Hp and polymeric Hp were calculated to be ~2.3 μM and ~2.0 μM, respectively. The corresponding value for unfractionated Hp could not be estimated due to the heterogeneity of this sample with respect to molecular mass. However, its molar concentration is expected to be between these calculated values.

The data in Figure 2A show that at approximately equivalent Hp concentrations, all three fractions of Hp bind HbO_2 at very similar speeds. We attempted to estimate quantitatively the rate constants for these bimolecular association reactions. HbO_2 in dilute solution is known to exist in equilibrium between the tetrameric and dimeric states [45]. The following expressions allow computation of the concentration of free dimers in our solutions:

$$K_{4,2}=\frac{[P_2]^2}{[P_4]};Y_{\mathrm{dim}er}=\frac{2[P_2]}{P_0};Y_{tetramers}=\frac{4[P_4]}{P_0}$$

$$\mathrm{K}_{4,2}=\frac{[P_2]^2}{[P_4]}=\frac{\left(\frac{1}{2}Y_{\mathrm{dim}er}P_0\right)^2_0}{\frac{1}{4}(1-Y_{\mathrm{dim}er})P_0}=\frac{Y^2_{\mathrm{dim}er}P_0}{(1-Y_{\mathrm{dim}er})}\Rightarrow Y^2_{\mathrm{dim}er}\frac{P_0}{\mathrm{K}_{4,2}}+Y_{\mathrm{dim}er}-1=0 \quad \text{Eq. 3}$$

$$Y_{dimer}=\frac{-1+\sqrt{1-4(P_O/K_{4,2})}}{2(P_O/K_{4,2})}$$

where Y_{dimer} is the fraction of HbO_2 dimers, P_O is the total Hb concentration in monomers equivalents, and $K_{4,2}$ is the HbO_2 tetramer-to-dimer dissociation equilibrium constant. Previous work [45] reported that $K_{4,2}$ is equal to approximately 1 μM in heme concentration in 0.1 M potassium phosphate buffer, pH 7.0 at 22 °C.

We mixed 0.05 mg/mL unfractionated Hp, dimeric Hp, or polymeric Hp with HbO_2 at 20 μM, 30 μM, 40 μM, and 50 μM heme concentrations in post-mixing heme equivalents. Following the analysis of Nagel and Gibson [41,42], the observed time courses for these rapid mixing reactions were then fitted to a single-exponential expression (i.e., Equation 1, with $y_2 = 0$). The observed pseudo first order rate constants for these reactions are plotted as a function of HbO_2 dimer concentration in Figure 2B. To construct these plots, we calculated the fraction of HbO_2 dimers present after mixing using Equation 3, then computed the concentration in dimeric units as $Y_{\mathrm{dimer}}P_0/2$ (Equation 3). The dimer concentrations in Figure 2B are 2.0, 2.5, 2.92, and 3.3 μM at 20, 30, 40, and 50 μM total heme concentrations post-mixing, respectively. Linear fits to the resulting data points yield slopes that approximate the second-order rate constant (k′) for the bimolecular association of

HbO_2 dimers with Hp αβ dimers. The values calculated from these slopes are presented in Table 1.

The calculated rate constants for these experiments suggest that the rates of HbO_2-Hp complex formation are very similar for the different Hp variants. This result indicates that the Hb binding sites and solvent accessibility of dimeric and polymeric forms of Hp are similar, if not identical. Our calculated association rate constants are all in the range of ~0.9 $\mu M^{-1}s^{-1}$, which agrees well with the value that was previously reported by Nagel and Gibson for experiments involving Hp 1-1 (i.e., ~0.5 $\mu M^{-1}s^{-1}$) using 0.1 M potassium phosphate buffer, pH 7.0 at 22 °C [42]. Cohen-Dix et al. [44] estimated a 10-fold smaller association rate constant (i.e., ~0.09 $\mu M^{-1}s^{-1}$) but used total heme concentration, did not correct for the amount of dimer present, and only looked at a single HbO_2 concentration.

Autooxidation and heme loss rates

It has been known anecdotally for many years that dilute solutions of oxygenated human Hb are much less stable than concentrated samples. In 1991, Zhang et al. [46] showed that the major cause is dissociation of HbO_2 into dimers, which then autooxidize ≥20-fold more rapidly than tetramers. This finding suggests that the binding of HbO_2 to Hp would also increase the rate of autooxidation, presumably because only Hb dimers bind to Hp. We verified this suggestion by measuring autooxidation of HbO_2 samples in the absence and presence of 2 equivalents of Hp (dimer) per 1 HbO_2 dimer as a function of total HbO_2 concentration (i.e. at 2.5, 5.0, 10, 50, and 100 μM in heme equivalents).

As shown in Figure 3A, the initial rate of autooxidation of free HbO_2 increases at least 15-fold, from ~0.02 hr^{-1} to ~0.3 hr^{-1}, when the heme concentration is decreased from 100 μM, where the protein is primarily a tetramer, to 2.5 μM, where it is roughly 50% dimers [46]. At the low protein concentration, the time course is probably biphasic, with each phase likely corresponding to non-equivalent autooxidation of the α and β subunits as suggested by Tsuruga and Shikama [47]. However, in order to examine the hemoglobin concentration dependences in consistent manner, we fit all the time courses to a single-exponent expression. An exact interpretation of these autooxidation times courses will require much more detailed study.

Our simple analysis of the time courses for all five different free HbO_2 solutions shows a progressive increase in the initial rate as the concentration is decreased 50-fold (Figure 3B). In contrast, when the HbO_2 is bound to Hp 1-1, a single phase is observed with an autooxidation rate constant of ~0.10 ± 0.03 hr^{-1} (Figure 3A), which does not vary with protein concentration (Figure 3B, dotted line), verifying that only Hb dimers bind to Hp. The solid line in Figure 3B for free HbO_2 was computed using the following expression:

$$k_{observed} = k_{autoox,dimer} Y_{dimer} + k_{autoox,tetramer}(1 - Y_{dimer}) \quad \text{Eq. 4}$$

where $k_{observed}$ is the fitted autooxidation rate at given HbO_2 concentration (P_0 in Equation 3); Y_{dimer} is the fraction of hemoglobin subunits in dimers, which was calculated using Equation 3; (1-Y_{dimer}) is the fraction of hemoglobin subunits in tetramers; and $k_{autoox,dimer}$ and $k_{autoox,tetramer}$ are the autooxidation rate constants for free Hb dimers and tetramers,

respectively. The solid line in Figure 3B was computed using $K_{4,2}$ = 1μM, $k_{autoox,dimer}$ = 0.4 h^{-1}, and $k_{autoox,tetramer}$ = 0.01 h^{-1}. The latter values are similar to those reported by Zhang et al. [46]. Thus, the extrapolated tetramer autooxidation rate constant is 40-fold smaller than that for free dimers.

Based on the data in Figures 3A and 3B, it is clear that Hb binding to Hp does speed up autooxidation roughly 10-fold compared to HbO_2 tetramers. However, the initial rate of autoxidation of the HbO_2-Hp(dimer) complex is still ~4-fold slower than the extrapolated rate of autooxidation of free HbO_2 dimers (Figure 3A), indicating that the hemoglobin dimer is stabilized by interaction with Hp compared to when it is free in solution.

Previous work by Bunn and Jandl [10,11] indicated that Hp binding to met-Hb impedes the transfer of heme from the resulting complexes to albumin, and that it abolishes radiolabeled heme exchange between met-Hb-Hp complexes and unbound met-Hb. Although this finding was recently corroborated by Lipiski et al. [12], who further reported equivalence between dimeric and polymeric Hp with respect to heme transfer to hemopexin, these findings controvert those of Bamm et al. [48]. The latter investigators reported that Hp 1-1 is more effective at attenuating heme release from Hb-Hp complexes than Hp 2-2 on the basis of studies with low-density lipoprotein [48]. We have investigated these findings further using the methods of Hargrove et al. [21], which offer the advantage of a spectrally unique apoMb reporter of heme loss.

Heme loss rates from met-Hb can be measured by co-incubating met-Hb with a heme-free Mb mutant (H64Y/V68F apoMb) which has a comparatively high affinity for heme and exhibits unique “green” visible light optical absorbance spectral properties following heme uptake [21]. Under conditions where H64Y/V68F apoMb is present in significant molar excess (i.e., ≥10-fold), heme dissociation from the met-Hb is normally irreversible due to rapid capture by the apoMb reagent [21]. This capture step results in the emergence of an optical absorbance peak at ~600 nm, and plotting absorbance changes at this wavelength as a function of time reveals the rate at which heme dissociates from met-Hb (Figure 3C).

We co-incubated either met-Hb alone or met-Hb-Hp complexes with H64Y/V68F apoMb and monitored visible light optical absorbance spectra over a four-hour period at 37 °C. Figure 3C shows absorbance time courses recorded at 600 nm. The absorbance changes for the control reaction containing met-Hb alone is biphasic and can be fit to the two exponential expression in Equation 1. The observed rate constants for free met-Hb are k_1 = ~9.2 hr^{-1} and k_2 = ~0.5 hr^{-1}, agree with literature values [21], and correspond to the rate of heme dissociation from met-Hb β and α subunits, respectively. In contrast, little or no increase in absorbance at 600 nm is observed when met-Hb-Hp complexes are reacted with H64Y/V68F apoMb. These results show that the rate of heme dissociation from met-HbA dimers bound to all three fractions of Hp is ≤ 0.01 hr^{-1} and that Hp binding almost completely inhibits heme dissociation on relevant physiological time scales (i.e., 1 to 24 hours; Figure 3C). Although our data corroborate those of Lipiski et al. [12], it is possible that the nonequivalence reported by Bamm et al. [48] could still be correct if low-density lipoprotein has a higher affinity for heme than hemopexin or H64Y/V68F apoMb.

Intrinsic redox potentials

The tendency of the iron centers in Hb to gain or lose electrons is reflected by their intrinsic redox potentials ($E_{½}$). This value is affected by the ligands binding to the iron in the first coordination sphere and the electronegativity of atoms in the second coordination sphere [32]. These Hb redox potentials are physiologically important because iron oxidation states influence both axial ligand binding (e.g., O_2) [27] and redox reactivity [2,5]. Additionally, $E_{½}$ measurements represent sensitive probes of distal pocket, porphyrin, and protein structural elements in Hb and other hemeproteins [49]. The red blood cell is a reducing environment, keeping the Hb iron centers in the 2+ oxidation state. However, following red cell lysis and dilution into plasma, Hb dissociates into dimers and can readily participate in redox chemistry [50]. We have recently shown that unfractionated Hp binding to Hb dimers can potentially short circuit this redox cycling by shifting the Hb $E_{1/2}$ to lower values [15]. This study showed that $E_{½}$ for free Hb is +124 ± 5 mV, whereas that for the dimer of Hb bound to Hp is +54 ± 2 mV [15]. These findings agree with previous $E_{½}$ measurements[51–53] and indicate a greater tendency of the heme iron centers within Hb-Hp complexes to be stabilized in the Fe(III) state than in free tetrameric Hb. Brunori et al. [54] previously studied Hb-Hp complexes prepared from fractionated forms of Hp and reported equivalent behavior for all the forms and redox potentials similar to those that we observe. However, more recent work has reported that Hp 1-1 mitigates Hb redox reactivity more effectively than Hp 2-2 [55]. In this study, we determined the $E_{1/2}$ values for the Hb-Hp(dimer) and Hb-Hp(polymer) complexes using a spectroelectrochemical method.

Figure 4 shows the variation in the absorbance peaks at the Soret region for a solution of Hb dimer bound to purified dimeric Hp as a function of applied electrode potential during a typical experiment. The isosbestic points at 415 nm, 455 nm, ~520 nm, ~610 nm, and ~660 nm indicate the presence of only two light-absorbing species, Fe(III)-heme and Fe(II)-heme. The relative concentrations of oxidized and reduced iron centers at each applied potential were calculated based on the absorbance intensities of the Soret peaks at 405 nm (Fe(III)-Hb) and 430 nm (Fe(II)-Hb), respectively. Nernst plots were obtained by plotting the log of the ratio $[Hb_{ox}:Hp]/[Hb_{red}:Hp]$ versus applied potential and are shown in Figure 5B. Equation 2 was fit to the resulting data points to determine the applied potential at which $[Hb_{red}:Hp] = [Hb_{ox}:Hp]$ and hence gives the value for $E_{½}$. Similar spectral behavior was observed for a polymeric Hp bound to Hb dimers (spectra not shown) and the Nernst plots for these species, along with unfractionated Hb-Hp, are shown in Figure 5. The resulting midpoint redox potentials for each sample are presented in Table 2. In agreement with the report of Brunori et al. [54], these data indicate that unfractionated Hp, dimeric Hp, and polymeric Hp exert similar effects on the $E_{½}$ values for bound Hb αβ dimers, reducing $E_{½}$ for the ferric/ferrous pair from ca +124 mV to ca +55 mV. The Hb dimer bound to Hp loses cooperative redox behavior as indicated by the linear nature of the Nernst plots compared to the non-linearity observed for free Hb tetramers. For all Hb-Hp complexes investigated the redox reaction is completely reversible. This indicates that although Hp stabilizes the Fe(III) state of the bound Hb dimers, it still binds with Fe(II) state strongly enough to retain the Hb-Hp complex. These data together suggest that Hp stabilizes “R-like”-state met-Hb during binding and that the effect is independent of the degree of Hp polymerization.

H_2O_2-induced ferryl species formation

Exposure of met-Hb to the endogenous oxidant H_2O_2 results in the formation of a ferryl heme species and a protein-based radical incident to H_2O_2 degradation [2,5]. This peroxidase or pseudo-peroxidase activity of Hb is believed to be enhanced by Hp binding [56], although the underlying mechanism is not fully understood. Hp binding to Hb dimers results in higher yields of detectable ferryl species and/or a decreased rate of their decay [15]. We sought to investigate whether the different forms of Hp exhibit similar behavior in this regard. Lipiski et al. [12] recently confirmed early findings by Nyman [57] that Hp 1-1 and Hp 2-2 behave similarly. However, Engler et al. [58] reported that Hb-Hp(1-1) complexes exhibit greater peroxidase activity than complexes prepared from Hp 2-1 or 2-2. We investigated this apparent discrepancy further using the methods of Berzofsky et al. [33].

One method of detecting and quantifying ferryl heme species involves the use of disodium sulfide (Na_2S) [33]. This reagent rapidly reacts with heme groups containing Fe(IV) atoms to produce a green product, sulfhemoglobin (sulf-Hb), which exhibits a strong and unique optical absorbance band with a maximum absorbance at ~617 nm [33]. The concentration of sulf-Hb in solution can be calculated using an extinction coefficient of 24.0 $mM^{-1}cm^{-1}$ at this wavelength [33]. Due to the specificity of the reaction between Na_2S and high-oxidation-state heme groups, sulf-Hb has routinely been used as a reporter for studying the transient generation of Fe(IV) oxo Hb species in biological samples and in vitro experiments [33].

We compared the effects of unfractionated Hp, dimeric Hp, and polymeric Hp on the formation of Fe(IV) oxo Hb species by oxidizing 10 μM met-Hb and met-Hb-Hp complexes to the Fe(IV) state using 20 μM H_2O_2. Following the H_2O_2 addition, samples were incubated for 2, 45, or 90 minutes at room temperature, after which catalase was added to degrade any remaining H_2O_2. Then, 20 μM Na_2S was mixed into each sample and optical absorbance spectra between 500 nm and 700 nm were recorded. Figure 6A contains sulf-Hb spectra of the samples from the 90 minute time point. As is evident by the absorbance peak at ~618 nm, these data show that sulf-Hb is present in all samples, with the greatest concentrations being present in the Hp-containing preparations. The sulf-Hb concentrations calculated from these spectra are 8.0 ± 0.1 μM, 7.9 ± 0.1 μM, and 8.1 ± 0.2 μM for the samples prepared with unfractionated Hp, dimeric Hp, and polymeric Hp, respectively, and 4.9 ± 0.1 μM for the sample containing met-Hb only. Data from the other time points are presented in Figure 6B, which consists of a plot of optical absorbance intensities at 618 nm against co-incubation times.

These data indicate that, at all time points investigated, the Hp-containing samples generated higher sulf-Hb concentrations than met-Hb alone. This finding agrees with our previous data using unfractionated Hp [15] and indicates that Hp binding modulates the reaction of Hb with H_2O_2 in a manner that stabilizes the ferryl Hb species. The new results in Figure 6 show that the fractionated forms of Hp all exert the same effects on Hb with respect to H_2O_2-induced Fe(IV) oxo species formation.

Radical formation

One method of studying the consumption of H_2O_2 by met-Hb is with the use of low-temperature electron paramagnetic resonance (EPR) spectroscopy. This method allows for the direct detection and quantification of the remaining high-spin ferric heme and protein-based radicals that are generated during this process [59]. We investigated whether met-Hb-Hp complexes prepared using unfractionated Hp, dimeric Hp, and polymeric Hp exhibit different behaviors regarding H_2O_2-induced radical formation.

Met-Hb and met-Hb-Hp complexes, were prepared as described in Materials and Methods and were treated with equimolar, 1.5-fold excess, and 5-fold excess H_2O_2. These samples were then incubated on ice for either 10 seconds or 60 seconds, and were quickly frozen before recording low-temperature EPR spectra. Spectra recorded at 10 K for Hb, Hp-Hp(dimeric), and Hb-Hp(poly) are shown in Figure 7. In the absence of H_2O_2, the addition of 0.1 M NaF uniformly converts these samples from a mixture of axial high-spin (g = 6 and 2) and rhombic low-spin (g_z =2.77 and g_y =2.25) heme signals into one that contains exclusively axial high-spin Fe. Treatment of met-Hb and met-Hp-Hp complexes with H_2O_2 results in a significantly diminished axial high-spin g = 6 EPR signal (~90% based on the g = 6 signal amplitude relative to that of the Hb-F complex) and development of stronger radical g = 2 signal. The radical yields calculated from double integration and normalized to a 1 mM copper standard are shown in Table 3. Expanded spectra for the protein radical g = 2 signal were recorded for additional samples at 115 K and are presented in Figure 8. Other than subtle differences in hyperfine splittings, the similar overall line width and total spin concentration reveal similar radical formation during the reaction of Hb with H_2O_2 when bound to the various Hp isoforms.

DISCUSSION

Hemolysis and the transfusion of banked blood or Hb-based therapeutics can result in varying quantities of circulating acellular Hb which can induce life threatening radical generating reactions in patients with a compromised vascular system [60]. Small to moderate levels of free Hb (<10 μM) have been reported to arise from transfused red blood cells and in sickle cell anemia [61]. In the case of Hb-based oxygen therapeutics, much larger quantities of free Hb are found in circulation. The later scenario has provided both the scientific and industrial communities a unique opportunity to examine closely the toxicity associated with acellular Hb in animals and in humans [62,63].

The pseudoperoxidase enzymatic activity of free Hb has been shown to trigger a cascade of lipid oxidation and downstream oxidative reactions [63]. Ferryl heme and associated protein radicals with high redox potentials (~1.0 V) can induce a wide variety of oxidative reactions that affect the protein and nearby molecules [2]. A number of specific oxidative changes have been reported to occur when the protein is reacted with excess H_2O_2 *in vitro*. First, the heme vinyl groups may become modified and covalently linked to the protein [64]. Second, extensive globin chain cross-links and irreversible modifications of several amino acids occur primarily in the “hotspots” of β subunits. Third, exposure to extracellular Hb, in the form of oxygen therapeutics or when Hb is released from old red blood cells, have also been reported to induce oxidative toxicity in kidney and brain tissues [65].

Biological systems express several globin and heme scavengers that can, under normal physiological states, deal effectively with acellular Hb in circulation [60]. Hp is the first-line scavenger that binds and accelerates the clearance of Hb in the circulation, although the macrophage CD163 receptor has also been the focus of several recent investigations [66–68]. New insights into the structure of the Hb-Hp complex have made it possible to examine the functional and structural interplay between the two proteins [7,69]. The crystal structure of porcine dimeric Hp-Hb complex revealed that the Hb-binding site is a putative serine protease domain, which contains several loops exposed on the surface and in the amino-terminal regions [7]. Amino acid residues in helices C, G and FG of both Hb subunits are part of the primary interface with Hp. These contacts are similar to those in the $\alpha_1\beta_2$ interface of the intact Hb tetramer. The crystal structure suggests that the Hb-Hp interaction may originate from an initial complex between the C-terminus of Hb α subunits and the active serine protease domain of Hp. Another striking finding from the crystal structure is that those amino acids on Hp which are susceptible to oxidation are in very close proximity to the Hb-Hp interface [66,70].

Whether oxidative side reactions initiated by Hb can be avoided or controlled in the Hp complex is a pivotal question under investigation in many laboratories. Identifying the region(s) that govern the interaction between Hb and Hp, and the affinity and specificity of each Hp fraction towards Hb is critical for the design of protective interventions against Hb toxicity in plasma. The degree to which Hp neutralizes the redox activity of the heme iron has been reported to differ among Hp phenotypes. This phenomenon has been shown in a number of systems both in vitro and in vivo [71]. Epidemiological studies appear to suggest that Hp 2-2 genotype is a risk factor for morbidity and mortality in a number of hemolytic conditions. This conclusion is based on the observation that the antioxidant capacity of the Hp 2-2 protein is decreased compared to the Hp 1-1 protein [16]. Further support for this hypothesis was obtained in cell culture media treated in an identical manner. The presence of increased redox activity was demonstrated in the plasma of transgenic Hp 2-2 diabetic mice compared with Hp 1-1 [71].

In this investigation we set out to examine the interactions between human Hb with fractionated Hp and in particular, the dimeric and polymeric forms. Hp samples were fractionated from pooled plasma, and native gel analysis suggested minimal cross contamination between monomeric and polymeric Hp fractions. We applied the methods of Nagel and Gibson [42] to study the kinetics of HbO_2 binding to Hp and found that unfractionated Hp, dimeric Hp and polymeric Hp bind HbO_2 dimers at almost identical rates. These data agree with the previously reported rates determined using Hp 1-1 [42], and show that all three fractionated forms of Hp fractions react rapidly with Hb dimers.

HbO_2 binding to Hp does speed up autooxidation roughly 10-fold due to dimerization. However, as shown in Figures 3A & 3B, the observed rate for dimers bound to Hp is still significantly slower than that of free HbO_2 dimers observed at low protein concentrations. Probably the most important Hp-mediated abrogation of Hb toxicity is stabilization of heme within the central cavity of the Hb subunits, which almost completely prevents its dissociation and subsequent free heme-mediated oxidative reactions and inflammatory responses. In previous work, Hp-Hb was shown to prevent heme transfer from Hb to LDL

[48]. Hp was also shown to prevent utilization of Hb iron by various pathogens [13]. We therefore examined heme loss kinetics from complexes of Hb with the dimeric and polymeric fractions and contrasted this with the unfractionated complexes of Hp using the H64Y/V68F apoMb heme-scavenging agent developed by Hargrove et al. [21].

When the met-Hb-Hp complex is mixed with the apoMb mutant, there is no detectable heme transfer after 6 hours as judged by the lack of change in the visible absorption spectrum of the mixture. In contrast, when free metHb is mixed with apoMb, the solution turns completely green after 4 hours, with the appearance of a strong peak at 610 nm indicative of heme transfer to form holo H64Y/V68F met-Mb (Figure 3C). Biphasic time courses are observed for free metHb. The rapid phase represents heme loss from β subunits and the slow phase heme loss from α subunits. When metHb dimers are bound to Hp, there is little or no loss of heme in the same time period from either unfractionated, dimeric or polymeric Hp complexes. Thus, the most dramatic effect of Hp binding to Hb is retention of heme, even after autooxidation of the iron. These experiments suggest that the overall affinity of apoHb bound to Hp for the oxidized form of heme is greater than or equal to that of the apoMb reagent ($K_D \ll 10^{-12}$ M [21,72]).

The high affinity of Hp for Hb dimers has two important implications. First, addition of exogenous Hp both markedly inhibits heme loss and second, as a result of this inhibition, globin precipitation is prevented. ApoHb denaturation occurs more rapidly at 37 °C when the heme is lost, but holoprotein is very stable under physiological conditions. As shown in Figure 3B, all three Hp fractions prevent heme dissociation from the corresponding met-Hb-Hp complexes. These findings are consistent with a recent study which showed that both Hp and hemopexin (heme scavenger) were equally effective in preventing vasoocclusion in a sickle cell mouse model infused with Hb [73]. In that study, heme was shown to specifically bind to endothelial Toll-like receptors (TLR4) and trigger a cascade of inflammatory responses, which could be attributed to oxidation and degradation of cell-free Hb [73]. Hp bound metHb and prevented heme loss and hemopexin captures any free heme released from metHb during its denaturation.

We also examined whether Hp fractions exhibit differences in their ability to suppress the redox activity of Hb in the presence of oxidants. We focused our attention on Hb pseudoperoxidase activity in the presence or absence of Hp fractions. Recent mechanistic experiments from our laboratory revealed that unfractionated Hp stabilizes the higher oxidation state of Hb (i.e., HbFe(IV)) and short-circuits subsequent radical-generating steps after exposure to oxidants such as H_2O_2. Ferryl Hb stabilization is accompanied by a significant increase in the concentration of the protein radical (•HbFeIV), likely on the penultimate tyrosine 145 of the Hb β subunit [74]. When Hp binds to Hb dimers, a sharp drop in the redox potential of the complex is observed. This negative shift in redox potential and its stabilized ferryl state appear to be the central element in how Hp protects against Hb-induced oxidative damage [15]. In this report we show that the redox potential of the Hb-Hp complex drops a constant amount no matter which Hp isoform is bound. This result indicates that Hb-Hp complexes have the same redox reactivities, regardless of the Hp phenotype. Additionally, the Nernst plots for Hb-Hp complexes show a loss of cooperativity

when compared to the plots for Hb and have slopes slightly less than one, indicating active-site heterogeneity (Table 2).

Our peroxidation data show that the initial stages of the iron reaction with H_2O_2 and subsequent ferryl formation within the heme pocket are not inhibited by the sequestration of Hb with Hp. In contrast to uncomplexed Hb, however, the ferryl species formed within the Hb-Hp complex was stabilized and persisted throughout the experiment. Using Na_2S to derivatize ferryl Hb into sulfHb, we were able to estimate the levels of ferryl Hb in these solutions. There was approximately twice as much sulfHb accumulated within the Hb-Hp complex irrespective of the size of the fractions as opposed to that of free Hb. This result is in accord with recent work, which showed that Hp binding to Hb prevents oxidative damage to the globin. The damage is instead redirected to Hp itself [74]. Hp has also been shown to stabilize ferryl Hb-associated protein radicals [74]. EPR experiments suggest that Hp might stabilize the protein radicals on tyrosine β–145, with possible subsequent migration to the Hp molecule [74]. In this study the stabilization of the ferryl form is also observed in our UV/Vis spectrophotometry experiments, but less stabilization of the protein radicals is seen in the current EPR study. The radical EPR spectra have line shapes typical for a protein tyrosyl radical and can be simulated as a tyrosyl radical with a “relaxed” conformation having a dihedral angle between the p_Z orbital of C1 and the Cβ hydrogen of the phenoxyl group ca. 30° [75]. However, determination of the exact protein location and detailed structure of the radical require combined site-directed mutagenesis, isotope replacements and EPR studies, which are beyond the scope of this study. Furthermore, the overall changes in EPR lineshape and signal size by Hp binding are marginal, thus the major stabilizing effects of Hp binding to Hb are almost complete inhibition of heme loss and reduction in the rate of autooxidation compared to free Hb dimers.

Another key conclusion is that the rate constants for the bimolecular association of Hb dimers are the same on all the forms of Hp under our experimental conditions. Similarly, heme loss does not occur rapidly from Hb-Hp complexes. The enzymatic ability of met-Hb to carry out redox cycling and consumption of H_2O_2 is also the same in all of the Hp complexes, as measured by the ability of each complex to stabilize ferryl heme and its associated protein radical. The genetic heterogeneity of human Hp isoforms has been reported to result in Hb-Hp complexes that differ in their binding and redox activities in vivo [16]. We do not presently have an explanation as to why in vitro data from our laboratory as well as others [12] reveal no major differences in either binding kinetics or redox properties of the different Hp fractions. Variability in the purification and fractionation processes of Hp into its major components may have contributed to non-equivalent behavior. It is also plausible that differences may be due to molecular mass differences which affect Hp distribution, clearance, and/or degradative pathways in vivo, or that the different isoforms of Hp have non-equivalent glycosylation which may result in functional differences under physiological conditions. Diverse methods have been used to characterize Hp activity, including those involving the use of linolenic acid, LDL, and hydrogen peroxide [71]. Although our data do not allow us to conclude that Hp genotypes on their own confer greater or lesser protection in isolation or as group, these biochemical findings should be taken into account when determining the role of heme-iron mediated vascular pathologies based on gene polymorphisms.

Acknowledgments

The authors thank Eileen Singleton for her efforts producing recombinant myoglobin, Francine Wood for assisting with Hb purification and catalase removal, Tigist Kassa for assistance at the bench, and Richard Chester from BPL for his assistance in Hp purification. The authors would like to also thank Dr. Dimitri A. Svistunenko of Essex University for helpful discussions related to the EPR measurements of the protein radical.

This work was supported by the National Institutes of Health (NIH) under grants HL110900 (AIA, JSO), HL095820 (A-LT), National Science Foundation Grant CHE 0809466 (ALC), Duke University (ALC), Welch Foundation Grant C-0612 (JSO), and by the U.S. Food and Drug Administration (MODSCI 2012, to AIA).

The abbreviations used are

EPR	electron paramagnetic resonance
Fe(III)	ferric iron
Fe(II)	ferrous iron
Fe(IV)	ferryl iron
Hb	hemoglobin
Hp	haptoglobin
met-Hb or met-Hb-Hp	Hb bearing Fe(III) alone or in complex with Hp, respectively
Hb or Hb-Hp complexes	deoxygenated Hb alone or in complex with Hp, respectively
NHE	normal hydrogen electrode
O_2	dioxygen
HbO_2	O_2-ligated Hb
sulf-Hb	sulfhemoglobin
$O_2^{\bullet-}$	superoxide radical
V	volts. We use the term heme to refer to protoporphyrin IX bearing either Fe(II) or Fe(III) for simplicity

References

1. Bunn, HF.; Forget, BG. Hemoglobin: molecular, genetic, and clinical aspects. Philadelphia: WB Saunders Company; 1986.
2. Reeder BJ. The redox activity of hemoglobins: from physiologic functions to pathologic mechanisms. Antioxid Redox Signaling. 2010; 13:1087–1123.
3. Shikama K. The molecular mechanism of autoxidation for myoglobin and hemoglobin: A venerable puzzle. Chem Rev. 1998; 98:1357–1373. [PubMed: 11848936]
4. Brantley RE Jr, Smerdon SJ, Wilkinson AJ, Singleton EW, Olson JS. The mechanism of autooxidation of myoglobin. J Biol Chem. 1993; 268:6995–7010. [PubMed: 8463233]
5. Rifkind JM, Ramasamy S, Manoharan PT, Nagababu E, Mohanty JG. Redox reactions of hemoglobin. Antioxid Redox Signaling. 2004; 6:657–666.
6. Bowman, BH.; Kurosky, A. Haptoglobin: The evolutionary product of duplication, unequal crossing over, and point mutation. In: Harris, H.; Hirschhorn, K., editors. Advances in Human Genetics. New York: Springer Science+Business Media LLC; 1982.

7. Andersen CBF, Torvund-Jensen M, Nielsen MJ, Oliveira CLP, Hersleth H-P, Andersen NH, Pedersen JS, Andersen GR, Moestrup SK. Structure of the haptoglobin-haemoglobin complex. Nature. 2012; 489:456–459. [PubMed: 22922649]
8. Kristiansen M, Graversen JH, Jacobsen C, Sonne O, Hoffman H-J, Law SKA, Moestrup SK. Identification of the haemoglobin scavenger receptor. Nature. 2001; 409:198–201. [PubMed: 11196644]
9. Allison AC, Rees W. The binding of haemoglobin by plasma proteins (haptoglobins). Br Med J. 1957; 2:1137–1143. [PubMed: 13472068]
10. Bunn HF, Jandl JH. Exchange of heme among hemoglobin molecules. Proc Natl Acad Sci U S A. 1966; 56:974–978. [PubMed: 5230192]
11. Bunn HF, Jandl JH. Exchange of heme among hemoglobins and between hemoglobin and albumin. J Biol Chem. 1968; 243:465–475. [PubMed: 4966113]
12. Lipiski M, Deuel JW, Baek JH, Engelsberger WR, Buehler PW, Schaer DJ. Human Hp1-1 and Hp2-2 phenotype-specific haptoglobin therapeutics are both effective in vitro and in guinea pigs to attenuate hemoglobin toxicity. Antioxid Redox Signaling. 2013; 19:1619–1633.
13. Eaton JW, Brandt P, Mahoney JR, Lee JT Jr. Haptoglobin: a natural bacteriostat. Science. 1982; 215:691–693. [PubMed: 7036344]
14. Jia Y, Wood F, Buehler PW, Alayash AI. Haptoglobin preferentially binds β but not α subunits cross-linked hemoglobin tetramers with minimal effects on ligand and redox reactions. PLoS ONE. 2013; 8:e59841. [PubMed: 23555800]
15. Banerjee S, Jia Y, Siburt CJP, Abraham B, Wood F, Bonaventura C, Henkens R, Crumbliss AL, Alayash AI. Haptoglobin alters oxygenation and oxidation of hemoglobin and decreases propagation of peroxide-induced oxidative reactions. Free Radical Biol Med. 2012; 53:1317–1326. [PubMed: 22841869]
16. Langlois MR, Delanghe JR. Biological and clinical significance of haptoglobin polymorphism in humans. Clin Chem. 1996; 42:1589–1600. [PubMed: 8855140]
17. Maeda N, Smithies O. The evolution of multigene families: human haptoglobin genes. Annu Rev Genet. 1986; 20:81–108. [PubMed: 2880559]
18. Levy AP, Asleh R, Blum S, Levy NS, Miller-Lotan R, Kalet-Litman S, Anbinder Y, Lache O, Nakhoul FM, Asaf R, Farbstein D, Pollak M, Soloveichik YZ, Strauss M, Alshiek J, Livshits A, Schwartz A, Awad H, Jad K, Goldenstein H. Haptoglobin: basic and clinical aspects. Antioxid Redox Signaling. 2010; 12(2):293–304.
19. Roche CJ, Dantsker D, Alayash AI, Friedman JM. Enhanced nitrite reductase activity associated with the haptoglobin complexed hemoglobin dimer: Functional and antioxidative implications. Nitric Oxide. 2012; 27:32–39. [PubMed: 22521791]
20. Dalton, J.; Podmore, A.; Kumpalume, P. Method for the Isolation of Haptoglobin. U.S. Patent Appl. 11/577,478.
21. Hargrove MS, Singleton EW, Quillin ML, Ortiz LA, Phillips GN, Olson JS, Mathews AJ. His64(E7)-->Tyr apomyoglobin as a reagent for measuring rates of hemin dissociation. J Biol Chem. 1994; 269(6):4207–4214. [PubMed: 8307983]
22. Wiedermann BL, Olson JS. Acceleration of tetramer formation by the binding of inositol hexaphosphate to hemoglobin dimers. J Biol Chem. 1975; 250:5273–5275. [PubMed: 238984]
23. Herbert D, Pinsent J. Crystalline human erythrocyte catalase. Biochem J. 1948; 43:203–205. [PubMed: 16748387]
24. Adamczyk M, Gebler JC. Electrospray mass spectrometry of alpha and beta chains of selected hemoglobins and their TNBA and TNB conjugates. Bioconjug Chem. 1997; 8:400–406. [PubMed: 9177847]
25. Aebi, H. [13] Catalase in vitro. In: Packer, L., editor. Methods Enzymol. Pennsylvania; Elsevier, Inc: 1984.
26. Banerjee R, Alpert Y, Leterrier F, Williams RJP. Visible absorption and electron spin resonance spectra of the isolated chains of human hemoglobin. Discussion of chain-mediated heme-heme interaction. Biochemistry. 1969; 8:2862–2867. [PubMed: 4309126]
27. Antonini, E.; Brunori, M. Hemoglobin and myoglobin in their reactions with ligands. Amsterdam: North-Holland Publishing Company; 1971.

28. Kurosky A, Barnett DR, Lee TH, Touchstone B, Hay RE, Arnott MS, Bowman BH, Fitch WM. Covalent structure of human haptoglobin: a serine protease homolog. Proc Natl Acad Sci U S A. 1980; 77:3388–3392. [PubMed: 6997877]
29. Ascoli, F.; Rossi Fanelli, MR.; Antonini, E. [5] Preparation and properties of apohemoglobin and reconstituted hemoglobins. In: Eraldo Antonini, LR-B., editor. Methods in Enzymology. Academic Press; New York: 1981.
30. Taboy CH, Bonaventura C, Crumbliss AL. Spectroelectrochemistry of heme proteins: effects of active-site heterogeneity on Nernst plots. Bioelectrochem Bioenerg. 1999; 48(1):79–86. [PubMed: 10228573]
31. Faulkner KM, Bonaventura C, Crumbliss AL. A spectroelectrochemical method for differentiation of steric and electronic effects in hemoglobins and myoglobins. J Biol Chem. 1995; 270(23): 13604–13612. [PubMed: 7775411]
32. Dhungana, S.; Crumbliss, AL. Spectroelectrochemistry. Kaim, W.; Klein, A., editors. Vol. Chapter 2. Royal Society of Chemistry; Cambridge, UK: 2008.
33. Berzofsky JA, Peisach J, Blumberg WE. Sulfheme proteins. I. Optical and magnetic properties of sulfmyoglobin and its derivatives. J Biol Chem. 1971; 246:3367–3377. [PubMed: 4324899]
34. Noble RW, Gibson QH. The reaction of ferrous horseradish peroxidase with hydrogen peroxide. J Biol Chem. 1970; 245:2409–2413. [PubMed: 5442280]
35. Mollan TL, Banerjee S, Wu G, Siburt CJP, Tsai A-L, Olson JS, Weiss MJ, Crumbliss AL, Alayash AI. α-Hemoglobin Stabilizing Protein (AHSP) markedly decreases the redox potential and reactivity of α-subunits of human HbA with hydrogen peroxide. J Biol Chem. 2013; 288(6):4288–4298. [PubMed: 23264625]
36. Kemmer G, Keller S. Nonlinear least-squares data fitting in Excel spreadsheets. Nature Protocols. 2010; 5:267–281.
37. Chiancone E, Alfsen A, Ioppolo C, Vecchini P, Agrò AF, Wyman J, Antonini E. Studies on the reaction of haptoglobin with haemoglobin and haemoglobin chains: I. Stoichiometry and affinity. J Mol Biol. 1968; 34:347–356. [PubMed: 5760461]
38. Okazaki T, Yanagisawa Y, Nagai T. Analysis of the affinity of each haptoglobin polymer for hemoglobin by two-dimensional affinity electrophoresis. Clin Chim Acta. 1997; 258:137–144. [PubMed: 9074811]
39. Adams EC, Weiss MR. Calorimetric studies of the haemoglobin-haptoglobin reaction. Biochem J. 1969; 115:441–447. [PubMed: 5353519]
40. Hwang PK, Greer J. Interaction between hemoglobin subunits in the hemoglobin-haptoglobin complex. J Biol Chem. 1980; 255:3038–3041. [PubMed: 7358726]
41. Nagel RL, Gibson QH. Kinetics and mechanism of complex formation between hemoglobin and haptoglobin. J Biol Chem. 1967; 242:3428–3434.
42. Nagel RL, Gibson QH. The binding of hemoglobin to haptoglobin and its relation to subunit dissociation of hemoglobin. J Biol Chem. 1971; 246:69–73. [PubMed: 5541775]
43. Alfson A, Chiancone E, Wyman J, Antonini E. Studies on the reaction of haptoglobin with hemoglobin and hemoglobin chains: II. Kinetics of complex formation. Biochim Biophys Acta, Protein Struct. 1970; 200:76–80.
44. Cohen-Dix P, Noble RW, Reichlin M. Comparative binding studies of the hemoglobin-haptoglobin and the hemoglobin-antihemoglobin reactions. Biochemistry. 1973; 12:3744–3751. [PubMed: 4788311]
45. Edelstein SJ, Rehmar MJ, Olson JS, Gibson QH. Functional aspects of the subunit association-dissociation equilibria of hemoglobin. J Biol Chem. 1970; 245:4372–4381. [PubMed: 5498425]
46. Zhang L, Levy A, Rifkind JM. Autoxidation of hemoglobin enhanced by dissociation into dimers. J Biol Chem. 1991; 266:24698–24701. [PubMed: 1761565]
47. Tsuruga M, Shikama K. Biphasic nature in the autoxidation reaction of human oxyhemoglobin. Biochim Biophys Acta. 1997; 1337:96–104. [PubMed: 9003441]
48. Bamm VV, Tsemakhovich VA, Shaklai M, Shaklai N. Haptoglobin phenotypes differ in their ability to inhibit heme transfer from hemoglobin to LDL. Biochemistry. 2004; 43(13):3899–3906. [PubMed: 15049697]

49. Olea C, Kuriyan J, Marletta MA. Modulating heme redox potential through protein-induced porphyrin distortion. J Am Chem Soc. 2010; 132:12794–12795. [PubMed: 20735135]
50. Buehler PW, Karnaukhova E, Gelderman MP, Alayash AI. Blood Aging, Safety, and Transfusion: Capturing the “Radical” Menace. Antioxid Redox Signaling. 2011; 14:1713–1728.
51. Antonini E, Wyman J, Brunori M, Taylor JF, Rossi-Fanelli A, Caputo A. Studies on the oxidation-reduction potentials of heme proteins I. HUMAN HEMOGLOBIN. J Biol Chem. 1964; 239:907–912. [PubMed: 14154472]
52. Abraham EC, Taylor JF. Oxidation-reduction potentials of human fetal hemoglobin and gamma chains. EFFECTS OF BLOCKING SUFHYDRYL GROUPS. J Biol Chem. 1975; 250:3929–3935. [PubMed: 236306]
53. Brunori M, Alfsen A, Saggese U, Antonini E, Wyman J. Studies on the oxidation-reduction potentials of heme proteins VII. OXIDATION-REDUCTION EQUILIBRIUM OF HEMOGLOBIN BOUND TO HAPTOGLOBIN. J Biol Chem. 1968; 243:2950–2954. [PubMed: 5653185]
54. Brunori M, Alfsen A, Saggese U, Antonini E, Wyman J. Studies on the oxidation-reduction potentials of heme proteins VII. OXIDATION-REDUCTION EQUILIBRIUM OF HEMOGLOBIN BOUND TO HAPTOGLOBIN. J Biol Chem. 1968; 243(11):2950–2954. [PubMed: 5653185]
55. Melamed-Frank M, Lache O, Enav BI, Szafranek T, Levy NS, Ricklis RM, Levy AP. Structure-function analysis of the antioxidant properties of haptoglobin. Blood. 2001; 98:3693–3698. [PubMed: 11739174]
56. Connell GE, Smithies O. Human haptoglobins: estimation and purification. Biochem J. 1959; 72(1):115–121. [PubMed: 13651145]
57. Nyman M. Serum hatoglobin; methodological and clinical studies. Scandinavian J Clin Lab Invest. 1959; 11(Supp 39)
58. Engler R, Rondeau Y, Pointis J, Jayle MF. Peroxydasic activities of hemoglobinic combinations of 3 haptoglobin phenotypes. Clin Chim Acta. 1973; 47:149–152. [PubMed: 4755799]
59. Svistunenko DA. Reaction of haem containing proteins and enzymes with hydroperoxides: The radical view. Biochim Biophys Acta, Bioenerg. 2005; 1707:127–155.
60. Buehler PW, Alayash AI. Oxidation of hemoglobin: mechanisms of control in vitro and in vivo. Transfusion Alternatives in Transfusion Medicine. 2007; 9:204–212.
61. Rother R, Bell L, Hillmen P, Gladwin M. The clinical sequelae of intravascular hemolysis and extracellular plasma hemoglobin: A novel mechanism of human disease. J Am Med Assoc. 2005; 293:1653–1662.
62. Silverman TA, Weiskopf RB. Hemoglobin-based oxygen carriers: current status and future directions. Transfusion. 2009; 49:2495–2515. [PubMed: 19903298]
63. Alayash AI. Oxygen therapeutics: can we tame haemoglobin? Nature Reviews Drug Discovery. 2004; 3:152–159.
64. Osawa Y, Darbyshire J, Meyer C, Alayash A. Differential susceptibilities of the prosthetic heme of hemoglobin-based red cell substitutes: Implications in the design of safer agents. Biochem Pharmacol (Amsterdam, Neth). 1993; 46:2299–2305.
65. Butt OI, Buehler PW, D’Agnillo F. Blood-Brain barrier disruption and oxidative stress in guinea pig after systemic exposure to modified cell-free hemoglobin. Am J Pathol. 2011; 178:1316–1328. [PubMed: 21356382]
66. Alayash A. Haptoglobin: Old protein with new functions. Clin Chim Acta. 2011; 412(7–8):493–498. [PubMed: 21159311]
67. Schaer DJ, Buehler PW, Alayash AI, Belcher JD, Vercellotti GM. Hemolysis and free hemoglobin revisited: exploring hemoglobin and hemin scavengers as a novel class of therapeutic proteins. Blood. 2013; 121:1276–1284. [PubMed: 23264591]
68. Subramanian K, Du R, Tan NS, Ho B, Ding JL. CD163 and IgG codefend against cytotoxic hemoglobin via autocrine and paracrine mechanisms. J Immunol. 2013; 190:5267–5278. [PubMed: 23589619]
69. Alayash AI, Andersen CBF, Moestrup SK, Bülow L. Haptoglobin: the hemoglobin detoxifier in plasma. Trends Biotechnol. 2013; 31:2–3. [PubMed: 23140673]

70. Schaer D, Buehler P, Alayash A, Belcher J, Vercellotti G. Hemolysis and free hemoglobin revisited: exploring hemoglobin and hemin scavengers as a novel class of therapeutic proteins. Blood. 2013; 121:1276–1284. [PubMed: 23264591]

71. Goldenstein H, Levy N, Levy A. Haptoglobin genotype and its role in determining heme-iron mediated vascular disease. Pharmacol Res. 2012; 66(1):1–6. [PubMed: 22465143]

72. Hargrove MS, Olson JS. The stability of holomyoglobin Is determined by heme affinity†. Biochemistry. 1996; 35:11310–11318. [PubMed: 8784185]

73. Belcher J, Chen C, Nguyen J, Milbauer L, Smith A, Nath K, Hebbel R, Vercellotti G. Hemin triggers vaso-occlusion in Murine sickle cell disease through activation of TLR4 signaling on endothelial cells. Blood. in press.

74. Cooper C, Schaer D, Buehler P, Wilson M, Reeder B, Silkstone G, Svistunenko D, Bulow L, Alayash A. Haptoglobin binding stabilizes hemoglobin ferryl iron and the globin radical on tyrosine beta 145. Antioxid Redox Signaling. 2013; 18(17):2264–2273.

75. Tsai A-L, Kulmacz RJ. Prostaglandin H synthase: Resolved and unresolved mechanistic issues. Arch Biochem Biophys. 2010; 493(1):103–124. [PubMed: 19728984]

Highlights

- Previous work correlates different isoforms of haptoglobin to different phenotypes
- This work involves studies of hemoglobin-haptoglobin binding and interactions
- Binding kinetics, heme loss, and redox reactions are similar between isoforms
  - Haptoglobin also modifies the autooxidation rate of bound hemoglobin dimers

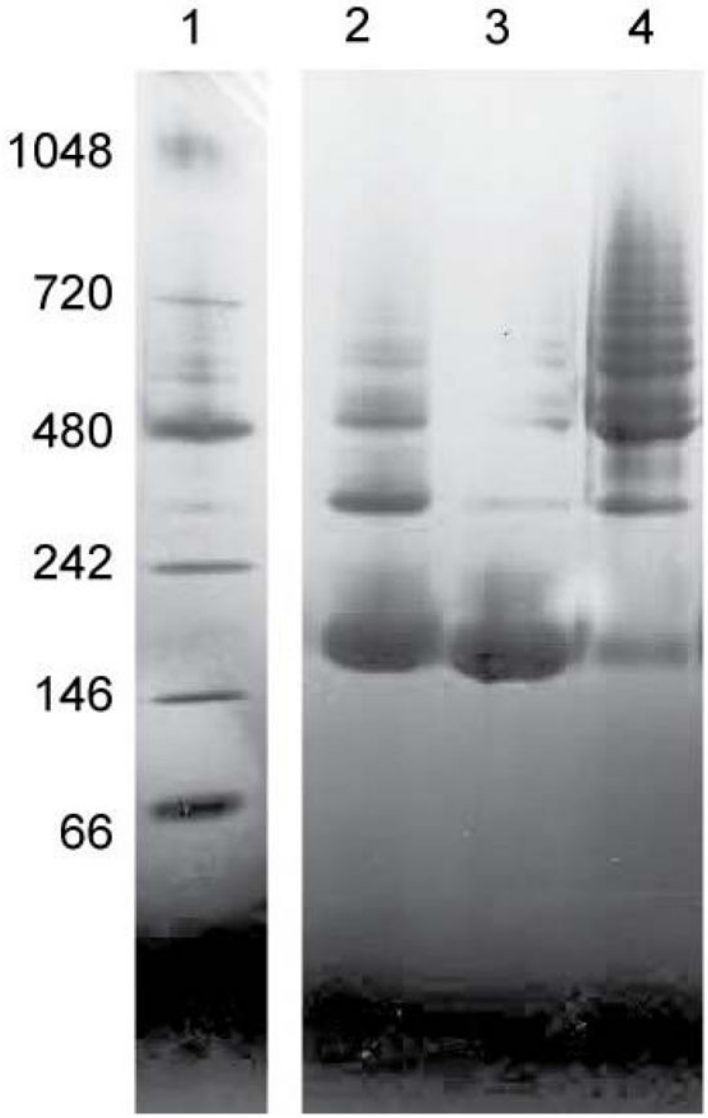

Figure 1.

Purity of fractionated forms of Hp. Samples were prepared in 50 mM potassium phosphate buffer, pH 7.4 at 22 °C and were loaded at the following concentrations and volumes: unfractionated Hp, 5 μL of 8 μM sample; and dimeric and polymeric Hp, 5 μL of 4 μM sample. Samples were run and gels prepared using the NativePAGE system by Invitrogen (Carlsbad, California, US) in accordance with instructions provided by the manufacturer. Lane 1 contains NativePAGE unstained marker, and Lanes 2, 3, and 4 contain unfractionated Hp, dimeric Hp, and polymeric Hp, respectively.

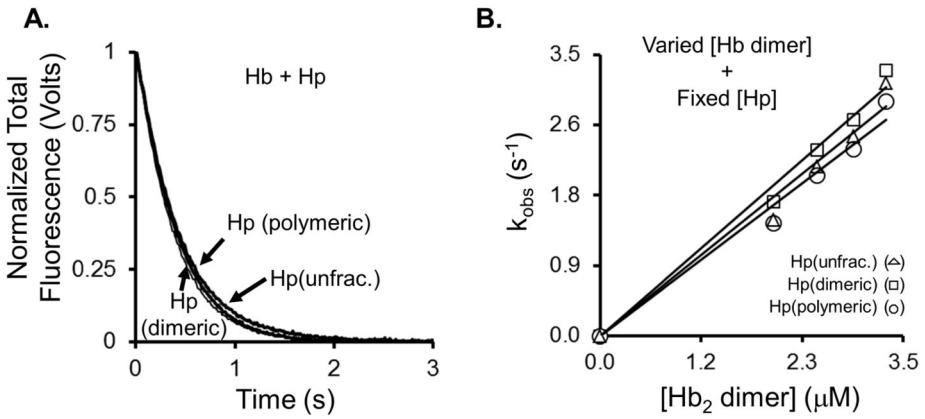

Figure 2.

Binding kinetics of HbO_2 with unfractionated, dimeric, or polymeric Hp. A, Representative time courses. B, Plot of observed rate constants for HbO_2-Hp association reaction. Total fluorescence changes as a function of time were measured by stopped-flow rapid mixing spectrophotometer using 50 mM potassium phosphate buffer, pH 7.4 at 22 °C. All fluorescence changes were normalized to total emission changes to correct for uniform intensity variations due to inner-filter effects. In Panel A, reactant concentrations are 80 μM HbO_2 in heme equivalents and 0.1 mg/mL unfractionated Hp, dimeric Hp, or polymeric Hp (pre-mixing concentrations). In Panel B, the x-ordinate units are given as Hb αβ dimer equivalents.

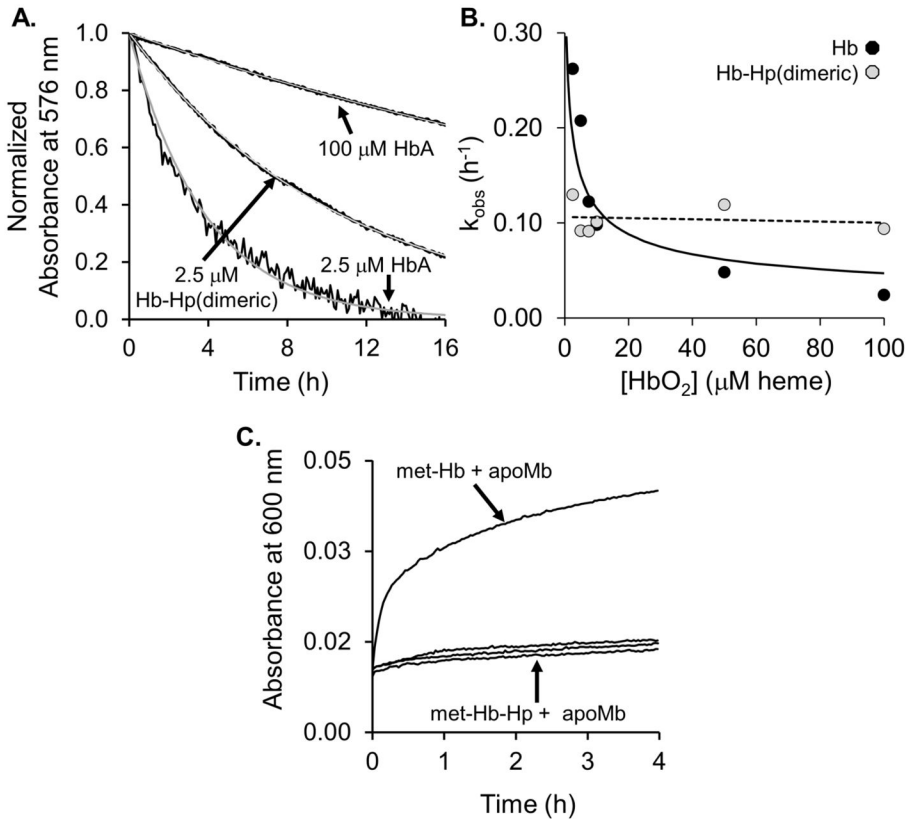

Figure 3.

Autooxidation and heme loss from Hb and Hb-Hp complexes. A, Representative time courses for the autooxidation of HbO_2 in the absence and presence of Hp(dimer) in 50 mM potassium phosphate, pH 7.4 at 37°C. Normalized absorbance decreases at 576 nm are shown using black lines and were fitted to a single-exponent expression (Equation 1, y_2 = 0), with the fits shown as gray lines. The fitted rate for 100 μM free HbO_2, is 0.02 h^{-1} and that for 100 uM HbO_2-Hp(dimer) is to 0.093 h^{-1}. The rate for autooxidation of 2.5 μM free HbO_2 is 0.26 h^{-1}. However, in the latter case, the fit to a one exponential expression is poor (see text). B, Plot of observed autooxidation rate constants versus Hb (monomer) concentration in the presence and absence of Hp(dimer). *Black circles* represent rates for free HbO_2; gray circles represent rates for HbO_2 bound to Hp(dimer). The solid line represents a fit to Equation 4 using $K_{4,2}$ = 1 μM, k_{autox}(dimer) = 0.40 h^{-1} and k_{autox} tetramer) = 0.01 h^{-1}. C, Time courses for heme loss at 37 °C using 200 mM potassium phosphate buffer, 600 mM sucrose, pH 7.0 at 22 °C. The absorbance changes at 600 nm are plotted as a function of time for these reactions. The time course for free met-HbA was fitted to a two exponential expression with rate constants equal to 9.4 and 0.50 hr^{-1} whereas time courses for the met-Hb-Hp complexes showed so little change that fitting was not possible even when much longer incubation times were used. Thus, the rate of heme dissociation from these complexes must be ≤ 0.01 h^{-1}.

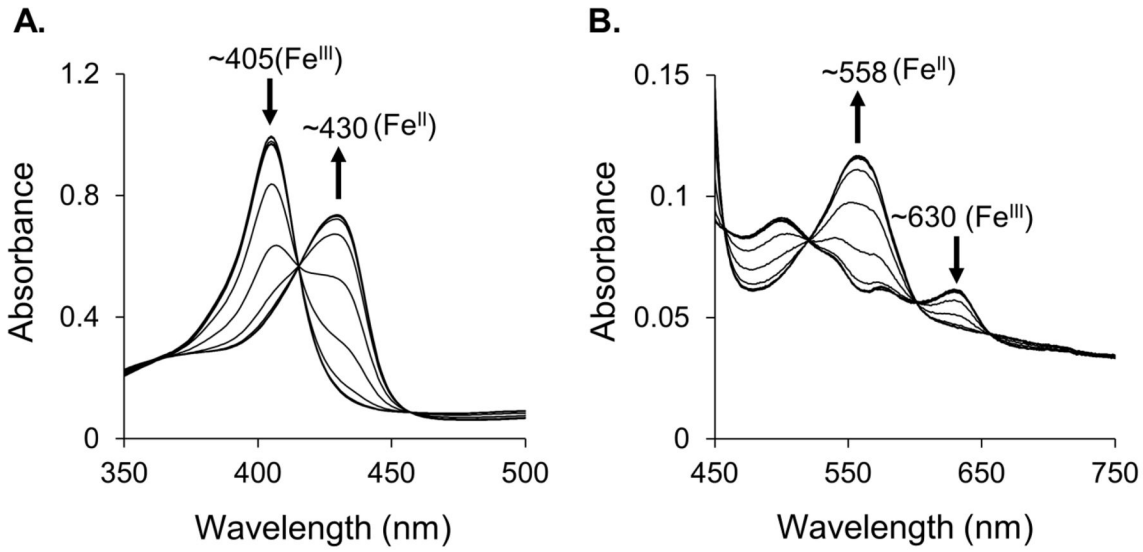

Figure 4.

Representative ferric and ferrous absorbance spectra during the positive-to-negative potential sweep for Hb-Hp(dimeric). A, The Soret optical absorbance peaks at ~405 nm and ~430 nm are indicative of met-Hb and Fe(II)-Hb, respectively. At increasingly negative potentials, the maximum at ~405 nm diminishes and an absorbance peak at ~430 nm emerges. Absorbance intensities at the Soret peaks were used to calculate the [Hb_{red}:Hp]:[Hb_{ox}:Hp] ratio. B, Heme oxidation state is also observed in the visible region. Arrows indicate the direction of absorbance change as the potential of the working electrode is made progressively negative. At the end of a negative potential sweep the scan direction was reversed, resulting in the regeneration of the original spectra. This indicates complete reoxidation of the heme moieties and shows that the redox process is reversible. Spectra recorded in 200 mM KPB buffer at pH 7.2 in the presence of 0.8 mM mediator. Panels A and B were both constructed using data from the same experiment.

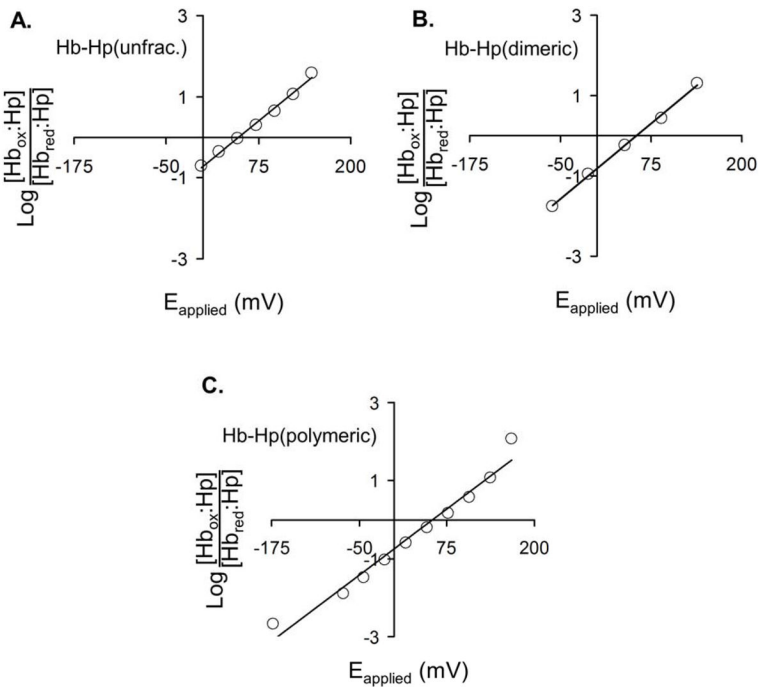

Figure 5.

Representative Nernst plots for A, Hb-Hp(unfractionated); B, Hb-Hp(dimer); and C, Hb-Hp(polymer) as obtained from separate spectroelectrochemistry experiments. Experiments were conducted using 200 mM potassium phosphate buffer, pH 7.2 at room temperature, and protein concentrations of 0.08 mM in heme equivalents. The open dots represent actual data points and the lines represent the best fit of Equation 2 to these data (see Materials and Methods). $E_{½}$ values calculated from multiple trials for each species are presented in Table 2.

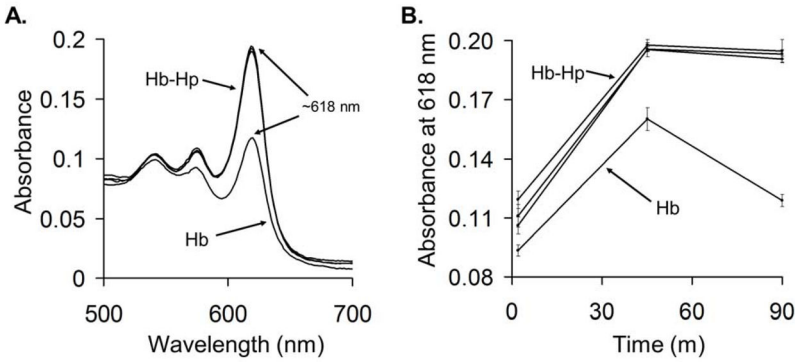

Figure 6.

Ferryl Hb species formation in H_2O_2-treated met-Hb and met-Hb-Hp complexes. A, Absorption spectra of sulf-Hb and sulf-Hb-Hp complexes. B, Concentration of sulf-Hb and sulf-Hb-Hp complexes as a function of H_2O_2 reaction time. In Panel A, 10 μM met-Hb or met-Hb-Hp complex were co-incubated with 20 μM H_2O_2 in 20 mM potassium phosphate buffer, pH 7.4 at 22°C, for 90 minutes prior to the addition of 200 units/mL of catalase. Then, 20 μM Na_2S was added to each sample and visible absorption spectra recorded. In Panel B, data from specific time points from this experiment are shown. Each data point is an average of three measurements. Error bars represent standard deviations. In Panel A, spectra corresponding to Hb-Hp samples appear superimposed due to overlap of the data sets.

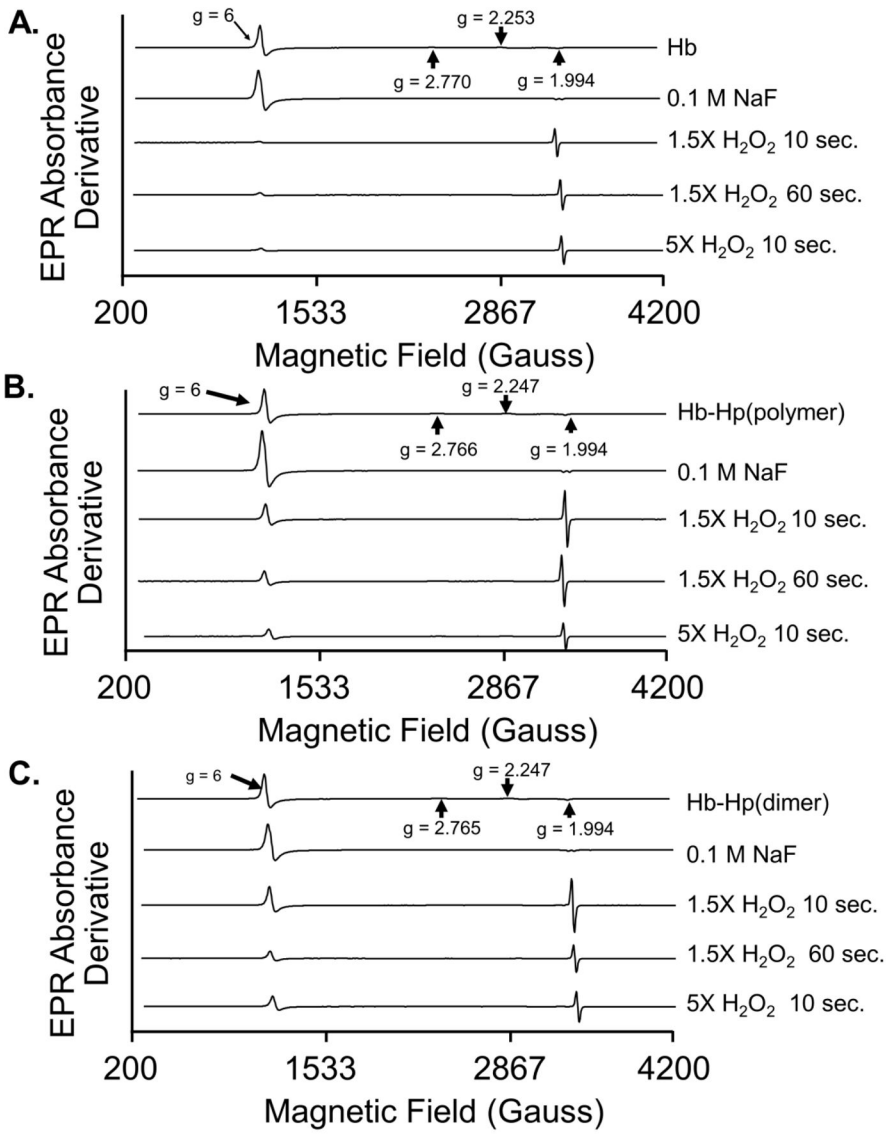

Figure 7.

Liquid He temperature EPR spectra of H_2O_2-treated met-Hb and met-Hb-Hp complexes. A, Hb in the absence of Hp. B, Hb-Hp(polymer) complexes. C, Hb-Hp(dimer) complexes. The buffer used for these spectra is 50 mM potassium phosphate buffer, pH 7.0 at 23°C. The instrument parameters corresponding to these spectra include: frequency, 9.58 GHz; power, 1 mW; and modulation frequency, 100 kHz; temperature, 10 K. The modulation amplitudes were 1 G for the samples containing met-Hb, met-Hb-Hp(unfract.), and met-Hb-Hp(dimer). The modulation amplitude was 2 G for the samples containing met-Hb-Hp(polymer). The spectra are normalized for different protein concentrations and modulation amplitudes.

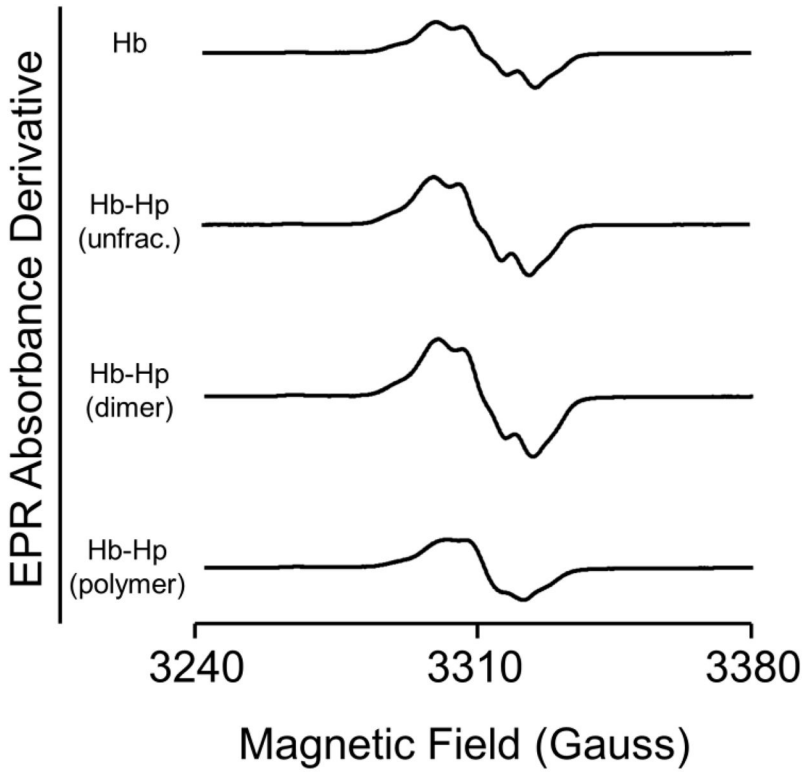

Figure 8.

Liquid N_2 temperature EPR spectra of H_2O_2-treated met-Hb and met-Hb-Hp complexes for the protein-derived radical. The buffer used for these spectra is 20 mM potassium phosphate buffer, pH 7.4 at 23°C. Instrument parameters: frequency, 9.285 GHz; power, 1 mW; modulation frequency, 100 kHz; modulation amplitude, 2.0 G; time constant: 327.7 ms; temperature, 115 K. Each spectrum represents one scan and is presented without normalization with the exception that the Hb-Hp(polymer) sample was normalized to 379 μM because the stock solution was more dilute than the other stock solution concentrations.

Table 1

Rate constants for bimolecular association of Hb dimers with binding sites on Hp. Each value was determined by averaging three reactions, with standard deviations for the fits contained in Figure 2B provided. 500 data points were collected for each reaction over the course of 5 seconds.

Hb + Hp	k' ($\mu M^{-1}s^{-1}$)
Hp (unfrac.)	0.9 ± 0.2
Hp (dimeric)	0.9 ± 0.1
Hp (polymeric)	0.8 ± 0.2

Table 2

Mid-point redox potentials ($E_{½}$) of Hb alone and in complex with the different Hp fractions. Measurements made using wild-type native Hb in 200 mM potassium phosphate buffer, pH 7.2 at 22 °C. All values reported here and in ref. 15 were performed in the same laboratory using the same apparatus and standardization methods, and represent a mean determined from triplicate experiments plus or minus (±) one standard deviation.

Sample	$E_{½}$ (vs NHE) (mV)
Hb ($\alpha_2\beta_2$ tetramers)†	+124 ± 5
Hb-Hp (unfractionated)†	+54 ± 2
Hb-Hp (dimeric)	+59 ± 2
Hb-Hp (polymeric)	+58 ± 2

†Values previously reported in Banerjee et al. [15] using 200 mM potassium phosphate buffer, pH 7.0 at 22 °C.

Table 3

Protein-based radical yields following treatment of Hb and Hb-Hp complexes with H_2O_2.

Samples	[protein]	[H2O2]	Reaction time	[spin] μM	Yield, %	Change[a] %
Hb	379 μM	1.5×	10s	10.7	2.8	100
Hb/dimer Hp				19. 5	5.1	181.5
Hb/unfrac. Hp				15.3	4.0	142.5
Hb/polymer. Hp	291 μM			7.7	2.7	93.6
Hb	80 μM	1×	150s	2.8	3.5	100
Hb/dimer Hp				4.9	6.2	178.7
Hb/unfrac. Hp				4.5	5.7	164.0
Hb/polymer. Hp				4.1	5.1	148.0
Hb		1.5×	10s	3.5	4.4	100
Hb/dimer Hp				2.5	3.1	69.4
Hb/unfrac. Hp				2.7	3.3	75.2
Hb/polymer. Hp				2.9	3.7	82.5
Hb			60s	3.6	4.5	100
Hb/dimer Hp				4.7	5.9	130.7
Hb/unfrac. Hp				4.2	5.3	117.3
Hb/polymer. Hp				3.7	4.6	101.6

[a]Relative amount of the spin, using the radical yield of Hb as 100%.